COMMTR

Communications in Transportation Research

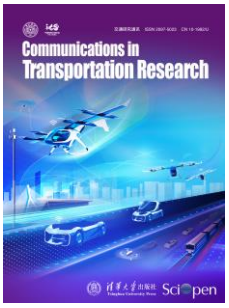

RESEARCH ARTICLE

Impacts of Closures of Critical Maritime Chokepoints on China's Trade and the Global Supply Chain

Zhan'ao Zhao[1, 3], Kai Liu[1, 2, 3]✉, Xiaoyi Miao[1, 3], Jiawang Zhang[1, 3], Ming Wang[1, 3]

1 Joint International Research Laboratory of Catastrophe Simulation and Systemic Risk Governance, Beijing Normal University, Zhuhai 519087, China.

2 Collaborative Innovation Center on Forecast and Evaluation of Meteorological Disasters (CIC-FEMD), Nanjing University of Information Science and Technology, Nanjing 210044, China.

3 School of National Safety and Emergency Management, Beijing Normal University, Beijing 100875, China.

✉ Corresponding author.

E-mail: liukai@bnu.edu.cn

DOI 10.26599/COMMTR.2026.9640075

Received 22 January 2026

Revised 26 May 2026

Accepted 23 November 2026

COMMTR Homepage

Cite this article: https://doi.org/10.26599/COMMTR.2026.9640075

Just Accepted

© The Author(s) 2026.

This is an open access article under the terms of the Creative Commons Attribution 4.0 International License (CC BY 4.0, http://creativecommons.org/licenses/by/4.0/), which permits use, distribution and reproduction in any medium, provided the original work is properly cited.

Published by **Tsinghua University Press**

https://www.sciopen.com/journal/2097-5023

清華大學出版社 Tsinghua University Press | SciOpen

Commun Transp Res

Research Article

Impacts of Closures of Critical Maritime Chokepoints on China's Trade and the Global Supply Chain

Zhan'ao Zhao[1, 3], Kai Liu[1, 2, 3]✉, Xiaoyi Miao[1, 3], Jiawang Zhang[1, 3], Ming Wang[1, 3]

Cite this article: xxx

ABSTRACT: China is deeply integrated into global supply chains, yet the dependence of China-related trade on critical maritime chokepoints, and the cascading impacts of their closure, remain unquantified. Here, we combine trade flows, maritime transport networks and multi-regional input–output linkages to assess closures at ten major maritime chokepoints. We find that closures of the Bab el-Mandeb Strait and the Suez Canal would substantially increase shipping costs and reduce trade flows, whereas closures of the Strait of Hormuz and the Bosporus Strait would interrupt trade because no viable alternative routes exist. These direct effects propagate through global supply chains: through backward and forward production linkages, every USD 1 of disrupted trade is associated with approximately USD 4.7 of gross output worldwide. Import disruptions propagate mainly upstream, with economies outside China bearing a disproportionate share of the effects. Export disruptions, in contrast, generate larger effects within China because export production is closely tied to domestic industries. Our results indicate that resilience strategies should focus on reducing closure probability and duration, while distinguishing between import- and export-side risks, to safeguard China-related trade and strengthen global supply-chain resilience.

KEYWORDS: international trade, maritime chokepoints, economic security, supply chains, trade disruption

Just Accepted

1 Introduction

China is the world's second-largest economy, largest industrial producer and leading trader in goods (Mi and Zhuang, 2022; Tan et al., 2025). In 2024, China imported USD 2.59 trillion in goods, the second-highest value globally, and exported USD 3.58 trillion, more than any other economy (General Administration of Customs of the People's Republic of China (GACC), 2025). China's large import demand provides a vast market for goods from around the world, while "Made in China" products can be found worldwide, supporting a diverse range of global demand. The scale of China's trade not only determines its important position in the global supply chain, but also means that any disruption to key trade with China could have a significant impact on the relevant countries and even the global economy (Berthou and Stumpner, 2024; Grossman et al., 2024; Tang and Zheng, 2024; Z. Xiao and Bai, 2022).

Maritime transport has long served as the primary mode for China's foreign trade, offering the advantages of massive carrying capacity and relatively low transportation costs. Nearly 90% of China's imports and exports by weight are transported by sea (Peng et al., 2025). This proportion also means that China's trade is highly exposed to the inherent risks of maritime transport. Although the ocean is vast, international shipping routes, constrained by geography, costs, and policy, are often funneled through a limited number of key maritime areas and narrow waterways. These zones serve as critical chokepoints within the global maritime network. Numerous shipping routes concentrated at critical chokepoints may carry goods connecting many countries, and the impact of blocked or closed routes will have a systemic effect on multiple countries and industries through trade and production networks (Kang et al., 2024; Verschuur et al., 2025; Winter and Scholz, 2024).

In 2021, the grounding of the Ever Given blocked the Suez Canal for nearly one week. More than USD 9 billion in global trade was disrupted each day, while 18 Chinese container and oil vessels were stranded. The blockage caused losses through delivery delays, higher transport costs and order cancellations (Feyrer, 2021; Li et al., 2025; Wan et al., 2023). Following the outbreak of the Russia–Ukraine war in 2022, traffic through the Bosporus Strait declined sharply, and global trade growth forecasts were revised downward from 4.7% to 2.4–3.0%. The sharp decline in grain exports from Russia and Ukraine has driven up global food prices and impacted China's grain and oil market (Arreyndip, 2025; Lin et al., 2023). In 2024, attacks on vessels in the Red Sea forced a large number of shipping routes to be diverted around the Cape of Good Hope. Shipping costs between the European Union and East Asia rose by approximately 20%, with China being the most significantly affected (Duan et al., 2024; Notteboom et al., 2024). More recently, in 2026, military escalation involving the United States, Israel, and Iran brought vessel traffic through the Strait of Hormuz to a near standstill. This has disrupted global energy markets and critical industrial supply chains (Zamani and Farzanegan, 2026).

Maritime disruptions have attracted increasing research attention.

[1] Joint International Research Laboratory of Catastrophe Simulation and Systemic Risk Governance, Beijing Normal University, Zhuhai 519087, China. [2] Collaborative Innovation Center on Forecast and Evaluation of Meteorological Disasters (CIC-FEMD), Nanjing University of Information Science and Technology, Nanjing 210044, China. [3] School of National Safety and Emergency Management, Beijing Normal University, Beijing 100875, China.

✉ Corresponding author. E-mail: **liukai@bnu.edu.cn**

Received: xxx xx, 20xx; Revised: xxx xx, 20xx; Accepted: xxx xx, 20xx

© The Author(s) 20xx. This is an open access article under the terms of the Creative Commons Attribution 4.0 International License (CC BY 4.0, http://creativecommons.org/licenses/by/4.0/).

Some studies have used trade data to construct networks of maritime trade flows with countries as nodes. By applying topological indicators, these studies analyzed changes in network structure under various shock scenarios, identified trade dependencies between countries, and provided a reference for formulating macro-level response strategies (Mesa-Arango et al., 2019; N. Wang et al., 2016; R. Xiao et al., 2024). With the increasing availability of Automatic Identification System (AIS) data, Geographic Information System (GIS) data, and liner schedule data, researchers have been able to construct increasingly realistic maritime transport networks. Related studies identify key ports or other important transportation nodes by simulating route planning or logistics allocation strategies, and analyze the cascading effects caused by the closure of these nodes (Dirzka and Acciaro, 2022; Pratson, 2023; Verschuur et al., 2022; Yan et al., 2021). For China, much of the literature concerns dependence on chokepoints for strategic commodity supplies and its implications for national economic security (Lee et al., 2025; J. Wang et al., 2023; X. Zhu et al., 2024). Grain imports, for example, pass through the Panama Canal, the Suez Canal, the Bosporus Strait, and the Strait of Malacca (L. Wang, 2015; W.L. Wang and Zeng, 2025). Strategic mineral imports depend heavily on the Strait of Gibraltar, the Suez Canal, the Strait of Hormuz, and the Strait of Malacca, among other passages (Bo et al., 2024; Xie et al., 2023).

These studies leave two questions insufficiently resolved. Analyses focusing on China's demand for specific commodities or on individual chokepoints capture only a part of the commodity composition and geographical distribution of China's maritime trade. Analyses of delays, congestion, and transport costs explain the logistics consequences, but rarely trace the affected goods through production and consumption in the economies involved. To address these limitations, we develop an analytical framework to connect chokepoint closures with the economic uses of the affected trade. It combines macro-level trade data, micro-level shipping networks, and the global multi-regional input–output (MRIO) structure. Using this framework, we simulate closure scenarios at ten key chokepoints worldwide. We then systematically quantify the additional transport costs, trade contractions, and cascading cross-economy effects associated with China-related trade under each scenario. The study aims to reveal the interdependence between China and the rest of the world in maritime trade. It also provides scientific evidence and policy insights for strengthening the resilience of global supply chains.

2 Data and methods

2.1. Trade–transport coupled network

Trade statistics come from the Trade-and-Transport Dataset (TTD) and the Base pour l'Analyse du Commerce International (BACI). TTD reports trade values and quantities for 170 economies and provides detailed information on transport mode and costs (Halim et al., 2018; Hoffmeister et al., 2022). BACI offers standardized bilateral trade flow data by processing UN Comtrade data (Gaulier and Zignago, 2010). For each trading partner, China-related records are extracted from both datasets. Maritime trade volumes from the TTD serve as the baseline. Where TTD values are missing or show large errors for certain regions, they are supplemented with BACI data.

To limit the influence of trade fluctuations driven by the COVID-19 pandemic, geopolitical conflicts, and trade frictions (Kazancoglu et al., 2023; Pratson, 2023; Xiong and Wu, 2021), we adopt 2019 as the baseline year. This is the most recent year for which all data sources are fully consistent, reflecting China's trade with the rest of the world under relatively normal conditions. In addition, we validate the framework using relevant data from 2021 and 2024 in the Supplementary Materials. The trade data cover 21 Harmonized System (HS) sections. We aggregate HS products into the first 11 sectors of EORA26 so that the trade data match the input–output table used in Section 2.3. HS codes are mapped to the International Standard Industrial Classification (ISIC Rev. 3) and then to EORA sectors, using the concordance tables of the World Bank's World Integrated Trade Solution (WITS).

Based on the constructed bilateral trade flows, we map China-related trade onto specific maritime routes. The global maritime network is derived from the International Shipping Lanes dataset developed by Oak Ridge National Laboratory (ORNL), which provides a spatial representation of major global shipping routes (Davis et al., 2026). Port locations and sector-specific cargo-handling capacities are obtained from Verschuur et al. (2022), who estimate port-level import and export capacities across sectors using vessel turnaround times and port-call frequencies. Integrating these two datasets, we select port pairs with matching sector-handling capacities as the origins and destinations for each sector, then apply Dijkstra's shortest-path algorithm (W. Zhu et al., 2022) to identify the cost-minimizing route between each pair within the global maritime network.

$$F_{pq}^{k} = T_{ij}^{k} \times \left(\frac{E_{i,p}^{k}}{\sum_{p} E_{i,p}^{k}} \right) \times \left(\frac{I_{j,q}^{k}}{\sum_{q} I_{j,q}^{k}} \right) \tag{1}$$

where F_{pq}^{k} denotes the trade flow of product k along the maritime route from port p to port q; T_{ij}^{k} denotes the total seaborne trade volume of sector k between economies i and j, one of which is China; $E_{i,p}^{k}$ and $\sum_{q} I_{j,q}^{k}$ denote the export capacity at port p and the import capacity at port q for sector k; and $\sum_{p} E_{i,p}^{k}$, $\sum_{q} I_{j,q}^{k}$ denote the corresponding total export and import capacities for sector k across all ports in the exporting and importing economies.

In total, we identify 1,289 ports across 212 economies with import–export linkages to China, and construct a global trade network covering 56,423 major maritime routes. Based on this network, we further estimate the trade volumes passing through key global maritime chokepoints. These estimates are also compared with independent external statistics in Supplementary Tables 4–5 to assess the reliability of the results.

2.2. Chokepoint closure scenario simulation

2.2.1 Additional cost calculation

To quantify the impacts of maritime chokepoint closures on China-related trade costs, we simulate closure scenarios. Under each scenario, the nodes and edges associated with a given chokepoint are removed from the baseline maritime network, preventing affected port pairs from using their original optimal routes (Supplementary Fig. 7); their reachability and alternative shortest paths within the remaining network are then re-evaluated. The resulting detours increase transport distances relative to the baseline, which in turn translate into changes

Just Accepted

in costs. All flows and costs are annual. A closure scenario is interpreted as a comparative-static closure lasting one year, and rerouting costs are computed for the annual cargo tonnage and value assigned to each port-pair route.

The specific procedure is as follows. First, using the preceding shortest-path results, we calculate the change in the shortest maritime distance between Chinese and foreign ports under each closure scenario, obtaining the additional rerouting distance L_c. Second, we estimate the potential delay caused by this distance increase. Each sector is matched with its corresponding vessel-type composition, including container ships, dry bulk vessels, general cargo vessels, RoRo vessels, and liquid bulk vessels (Ligteringen and Velsink, 2012; Martínez et al., 2015). Since different vessel types have different sailing speeds, distance costs, and time costs, we calculate the weighted average vessel speed, weighted unit distance cost, and weighted unit time cost for each sector according to the vessel-type transport shares shown in Supplementary Table 1. For sector i, the delay time t_i is obtained by dividing the additional distance L_c by the weighted average vessel speed s_i.

Third, for sector *i*, this cost consists of three components: distance-based transport costs from the longer sailing distance, time-based operating costs from the longer transit time, and value-of-time losses from cargo delays:

$$Cost_i = q_i \cdot L_c \cdot c_i^d + t_i \cdot q_i \cdot c_i^t + VOT_i \cdot v_i \cdot \frac{t_i}{24} \tag{2}$$

where q_i and v_i denote the transported weight and trade value of sector *i*, respectively, and c_i^d, c_i^t and VOT_i denote the unit distance cost, unit time operating cost, and value-of-time coefficient for that sector, respectively. The specific parameter values are provided in Supplementary Tables 2–3.

Fourth, the results are aggregated at the route level. Since a single route usually carries multiple cargo types, route-level delay time is calculated as the cargo-weighted average delay across sectors:

$$t_{mean,r} = \frac{\sum_{i=1}^{11} t_{i,r} q_{i,r}}{\sum_{i=1}^{11} q_{i,r}} \tag{3}$$

The total additional cost at the route level is obtained by summing the additional costs of all 11 sectors:

$$Cost_{route,r} = \sum_{i=1}^{11} Cost_{i,r} \tag{4}$$

Fifth, the results are aggregated at the chokepoint level. For each closure scenario, we combine all affected port pairs that can still be rerouted and calculate the cargo-weighted average delay and the total additional cost. Because the costs are calculated from the annual tonnage and value on each route, these totals are annual costs, not per-voyage costs.

The mix of vessel types used for each cargo sector is uncertain, which affects sailing speed, transit time, and transport costs. To account for this, we randomly sample vessel-type shares within predefined sector-specific ranges and run repeated Monte Carlo simulations (Balas and Balas, 2025). The results are reported as distributions, including quantiles, means, standard deviations, and coefficients of variation.

2.2.2 Trade contraction calculation

Higher costs also cut trade. Once the added cost is large relative to the value of the goods, part of the trade is no longer worth shipping. We model this endogenous adjustment with the iceberg trade-cost assumption and the trade-cost elasticity implied by the structural gravity model (Bergstrand et al., 2013; Head and Mayer, 2014). We assume that the trade flow Q and the trade-cost factor τ follow a power-law relationship:

$$\frac{Q_1}{Q_0} = \left(\frac{\tau_1}{\tau_0}\right)^{\varepsilon} \tag{5}$$

where Q_0 and Q_1 denote the trade flow before and after the closure, respectively, and τ_0 and τ_1 denote the corresponding trade-cost factors. $\varepsilon < 0$ is the trade-cost elasticity, indicating that trade flow declines nonlinearly as trade cost rises. Existing studies suggest that this parameter typically lies between −3 and −6 (Head and Mayer, 2014; Simonovska and Waugh, 2014); we adopt this range for sensitivity analysis to assess the robustness of the estimated trade contraction and gross-output effects to parameter uncertainty.

To apply this general relationship to specific chokepoint closure scenarios, we examine the transport-cost shock faced by the trade flow of country *c* and sector *s* through chokepoint *K*: once the chokepoint closes, cargo rerouted via alternative paths incurs an additional detour cost, giving rise to a corresponding effective ad valorem trade-cost shock $\Delta\tau$. The trade-cost factors before and after closure, and the corresponding cost shock, can be expressed respectively as:

$$\tau_0 = 1 + \frac{C_{K,c,s}^{\text{base}}}{v_{c,s}} \tag{6}$$

$$\tau_1 = 1 + \frac{C_{K,c,s}^{\text{base}} + C_{K,c,s}^{\text{reroute}}}{v_{c,s}} \tag{7}$$

$$\Delta\tau_{K,c,s} = \frac{C_{K,c,s}^{\text{reroute}}}{v_{c,s} + C_{K,c,s}^{\text{base}}} \tag{8}$$

where $C_{K,c,s}^{\text{base}}$ denotes the original transport cost under normal conditions, $C_{K,c,s}^{\text{reroute}}$ denotes the additional transport cost incurred by rerouting after chokepoint closure and $v_{c,s}$ denotes the trade value carried through that chokepoint. Substituting this cost shock into the trade-cost–flow elasticity relationship above yields the first-order trade-contraction ratio resulting from the rise in transport cost:

$$\sigma_{K,c,s} = 1 - \left(1 + \Delta\tau_{K,c,s}\right)^{\varepsilon} \tag{9}$$

where $\sigma_{K,c,s}$ denotes the effective contraction ratio of the trade flow of country *c* and sector *s* resulting from the transport-cost increase following closure of chokepoint *K*. σ is set to 100% where closure leaves no feasible alternative maritime route; where only some port pairs are cut off, this trade is assigned the contraction ratio of the corresponding partner–sector flow.

2.3. Economic impact assessment

2.3.1 Trade flow–MRIO coupling

Chokepoint closure triggers cascading shocks across upstream and downstream industries through inter-industry input–output linkages. To capture this transmission mechanism, we extend the framework of Verschuur et al. (2022), linking China-related maritime trade flows to

Just Accepted

the MRIO system and tracing closure impacts down to the chokepoint level. For each trade flow passing through target port p and target chokepoint K (exporting economy $c_{\exp}$, importing economy c_{imp}, sector i), its relative weight within the MRIO coordinate system is uniquely defined by the parameter s_{trade}:

$$S_{trade,K}^{(p,c_{exp},c_{imp},i)} = \omega_p^{(c_{exp},c_{imp},i)} \times \mu^{(c_{exp},c_{imp},i)} \times \varphi_K^{(c_{exp},c_{imp},i)} \quad (10)$$

where ω_p denotes the value share carried by port p in maritime trade for that country pair and sector, and μ denotes the share of maritime transport in total trade for that country-sector pair. φ_K denotes the share of maritime trade routed through chokepoint K.

This study uses the EORA26 MRIO database. For each economy, we extract 11 of the 26 sectors, namely the goods-producing sectors. Table 1 summarizes the core parameters of the framework, together with their sources or calculation methods.

Table 1. Definitions and data sources of key input–output variables

Symbol	Definition	Data source / Formula
A	Technical coefficient matrix	EORA26
Z	Intermediate input matrix	EORA26
Y	Final demand matrix	EORA26
D	Domestic final demand vector	Sum the specified columns of Y by sector.
E	Sectoral export vector	Aggregate intermediate exports from the home economy to all foreign economies in Z by sector.
X	Original total output vector	EORA26
B	Ghosh allocation coefficient matrix	$B = \hat{X}^{-1} \cdot Z$, where $\hat{X}$ is the diagonal matrix of total output.
v	Value-added row vector	$v = X \cdot (I - B)$, treated as constant.

2.3.2 Import impact indicators

Import impact indicators quantify the extent to which commodities imported through a given port or chokepoint support final consumption and re-exports in the importing economy. The calculation proceeds in four steps. We begin with a zero-filled sparse matrix A' of the same dimensions as A. For a route through the selected port or chokepoint $(c_{\exp}, i, c_{imp})$, the corresponding coefficient in A is weighted by the route's trade share s_{trade} and entered into A'. This yields the import input coefficients attributable to a specific trade flow, as defined in Eq. (11). In this way, the trade flow under examination is extracted from the global MRIO framework.

$$A'^{(c_{exp},i,c_{imp})} = A^{(c_{exp},i,c_{imp})} \cdot S_{trade}^{(c_{exp},c_{imp},i)} \quad (11)$$

Second, in A', import contributions from all foreign origins are summed by column to obtain, for the importing economy c_{imp}, the sectoral j import coefficient vector L, as specified in Eq. (12). L is an 11 × 1 vector; its j-th component denotes the share of intermediate inputs in country c_{imp} sector j that is imported from all foreign economies through the port or chokepoint.

$$L_j^{(c_{\text{imp}})} = \sum_{c_{\exp} \neq c_{\text{imp}}} \sum_i A'^{(c_{\exp},i,c_{\text{imp}},j)} \quad (12)$$

Third, L is multiplied by the domestic Leontief inverse $(I - A_{dom})^{-1}$ to obtain the import demand vector M, which incorporates indirect effects through domestic industrial linkages, as specified in Eq. (13). Here, A_{dom} denotes the domestic sector-to-sector coefficient submatrix of A for country c_{imp}, an 11 × 11 matrix. Its Leontief inverse captures the indirect output across all sectors induced by one unit of final demand in country c_{imp}. Thus, M represents the total import demand from the trade flow embodied in each unit of final output under full domestic supply-chain transmission.

$$M^{(c_{imp})} = L^{(c_{imp})} \cdot \left(I - A_{dom}^{(c_{imp})}\right)^{-1} \quad (13)$$

Fourth, M is dotted with the sectoral export vector E and the domestic final-demand vector D to obtain two measures of import demand:

$$M_{exp}^{(c_{imp})} = M^{(c_{imp})} \cdot E^{(c_{imp})} \quad (14)$$

$$M_{dom}^{(c_{imp})} = M^{(c_{imp})} \cdot D^{(c_{imp})} \quad (15)$$

2.3.3 Export impact indicators

To characterize the mechanisms through which trade-flow reductions affect global output, we develop export-impact indicators from three perspectives: intermediate inputs, final demand, and the supply side. These indicators assess backward (upstream) and forward (downstream) linkages, with the trade-contraction ratio σ resulting from chokepoint closure set according to the actual cost increase at each chokepoint.

Assume that the share of a given trade flow in the relevant country-pair-sector–chokepoint intermediate input is s_{trade}. Under trade contraction scenario σ, the corresponding cell in the technical coefficient matrix A is reduced by $(1 - s_{\text{trade}} \cdot \sigma)$, yielding the adjusted coefficient matrix A^*:

$$A^{*(c_{\exp},i,c_{\text{imp}})} = A^{(c_{\exp},i,c_{\text{imp}})} \cdot \left(1 - s_{\text{trade}} \cdot \sigma\right) \quad (16)$$

This formula modifies only the element $(c_{\exp}, i, c_{imp})$ of A that corresponds to this trade flow, while all other elements remain unchanged. Economically, the disrupted maritime trade reduces the demand of production sectors in country c_{imp} for intermediate inputs from country $c_{\exp}$ sector i in proportion to the contraction ratio. Using A^*, the Leontief inverse is recalculated and applied to the original final demand Y_0, yielding the new total output under the A-shock.

$$X_A^* = \left(I - A^*\right)^{-1} \cdot Y_0 \quad (17)$$

Trade contraction also reduces final consumption by the importing economy c_{imp} of goods from country $c_{\exp}$ sector i. Accordingly, the corresponding cell in the final-demand matrix Y is reduced by $(1 - s_{\text{trade}} \cdot \sigma)$, yielding the adjusted Y':

$$Y'^{(c_{\exp},i,c_{\text{imp}})} = Y^{(c_{\exp},i,c_{\text{imp}})} \cdot \left(1 - s_{\text{trade}} \cdot \sigma\right) \quad (18)$$

With A unchanged, the original Leontief inverse $\left(I - A\right)^{-1}$ is applied to the adjusted final-demand matrix to obtain the new total

Just Accepted

output under the Y-shock X_Y^*.

$$X_Y^* = (I - A)^{-1} \cdot Y' \tag{19}$$

The output differences generated by the two shocks are then combined to obtain the backward industrial impact of the trade flow ΔX_{BW}.

$$\Delta X_{BW} = (X_0 - X_A^*) + (X_0 - X_Y^*) \tag{20}$$

Forward shocks are characterized using the Ghosh model. The Ghosh allocation coefficient matrix $B = \hat{X}^{-1} Z$ represents the allocation of sectoral output between intermediate and final uses. Under scenario σ, the corresponding cell in B is reduced in the same manner to obtain B^*:

$$B^{*(c_{\exp}, i, c_{\text{imp}})} = B^{(c_{\exp}, i, c_{\text{imp}})} \cdot (1 - s_{\text{trade}} \cdot \sigma) \tag{21}$$

The pre-computed value-added row vector v is then multiplied by $(I - B^*)^{-1}$ to obtain the new total input under the supply-side shock X_B^*:

$$X_B^* = v \cdot (I - B^*)^{-1} \tag{22}$$

X_B^* represents the total input required from each sector after changes in the supply-side allocation structure. Its difference from the original X_0 captures the output contraction in downstream sectors caused by the reduction in this trade flow. In addition, the forward shock includes the loss on the final-consumption side $\Delta \mathbf{C}_{\text{FW}}$, namely the direct loss of final consumption due to reduced trade:

$$\Delta \mathbf{C}_{\text{FW}} = \sum_{c_{\exp}, i, c_{\text{imp}}} Y^{(c_{\exp}, i, c_{\text{imp}})} \cdot s_{\text{trade}} \cdot \sigma \tag{23}$$

The two components are combined to obtain the forward industrial impact ΔX_{FW}, which captures both the output contraction in downstream sectors that use this traded commodity as an input and the direct loss of final consumption caused by reduced consumer-goods supply:

$$\Delta X_{FW} = (X_0 - X_B^*) + \Delta C_{FW} \tag{24}$$

The sum of the forward and backward effects gives the total gross-output effect of the disruption of this trade flow:

$$\Delta X_{total} = \Delta X_{BW} + \Delta X_{FW} \tag{25}$$

Eqs. (16)–(25) apply hypothetical extraction. The disrupted flow is removed from the inter-industry matrix and from final demand, and the resulting change in gross output is evaluated from the demand side (Eqs. 16–20) and the supply side (Eqs. 21–24). The total effect combines the flow-dependent output of upstream suppliers and that of downstream users. Each of these two components includes the disrupted flow itself as its direct effect. Dividing the total effect by the value of disrupted trade gives the gross-output exposure multiplier. This multiplier indicates how much production is exposed to the disruption, rather than the resulting loss of GDP.

3 Results

3.1. China's trade structure and chokepoint identification

China's foreign trade covers a wide range of economies and products. Trade data show that China maintains import and export relations with about 85% of the world's economies, and its trade products cover about 98% of the commodity categories in global trade.

East Asia and the Pacific supply about 49% of China's imports by value, and Europe and Central Asia 21%; no other region exceeds 9% (Fig. 1a). On average, China imports from about 139 economies per sector. Sectors with higher import values also tend to have more source economies (Fig. 1b). To measure how concentrated the sources are, we sort the source economies in each sector by trade share, from smallest to largest, and compute cumulative shares. Two patterns emerge. In the first, a sector is sourced from many economies but dominated by a small number of suppliers. In Fig. 1b, this appears as a narrow gap between the cumulative shares at the 50th and 90th percentiles. For example, China imports vegetable products from around 140 economies, but Brazil alone accounts for 38% of the total import value. Leather products are imported from 145 economies, of which Italy accounts for approximately 25%. The second pattern is characterized by more concentrated sourcing, with imports coming from fewer economies and one or a few suppliers accounting for a large share. In Fig. 1b, this pattern is reflected in the close proximity of the cumulative shares at the 10th and 50th percentiles. Footwear and headwear products are sourced from around 122 economies, yet Vietnam alone accounts for 47% of the total import value. Animal and vegetable oils and fats are sourced from only 98 economies, of which Indonesia contributes approximately 40%. Supplementary Table 11 reports the main source economies and their shares for each import sector.

On the export side, China reaches a broader range of markets. The average sector ships to about 200 economies. By value, 36% of exports go to East Asia and the Pacific, 24% to Europe and Central Asia and 21% to North America. For most sectors, when destinations are ranked by export value in ascending order, the cumulative shares at the 50th and 90th percentiles differ slightly. A few large buyers thus sit on top of a long tail of small markets (Fig. 1b). The United States, Japan, South Korea, and Germany are the major destinations for most sectors (Supplementary Table 11). The United States takes about 20% of China's exports; no other destination exceeds 10%.

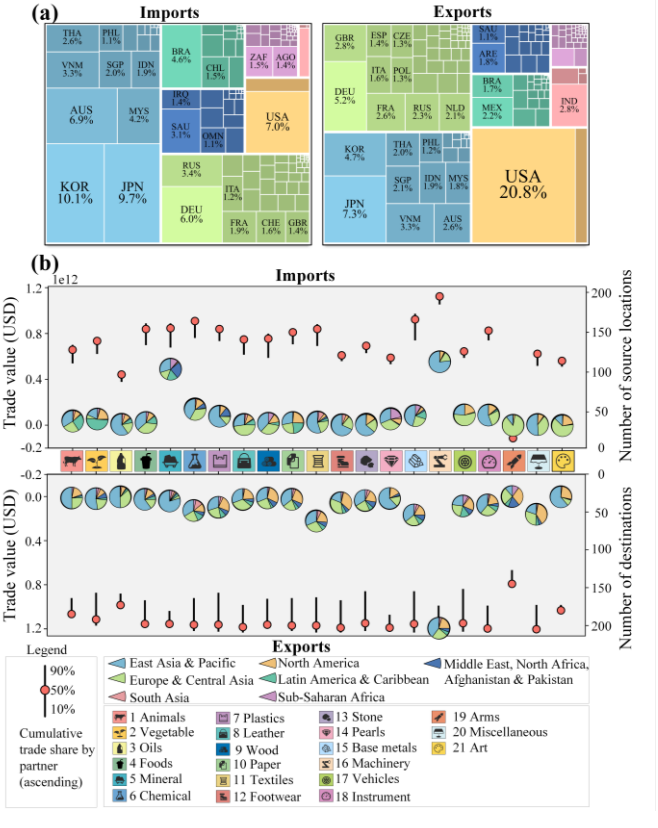

Just Accepted

Fig. 1 China's import and export trade pattern. (a) Breakdown of China's total imports and exports across partner economies, grouped by region. Letters indicate the ISO 3166-1 alpha-3 (ISO3) codes of countries or regions. Hong Kong, Macao and Taiwan are excluded. (b) Statistical characteristics of China's import and export product categories and their source and destination economies.

China's maritime trade with major global economies is concentrated along two trunk routes: the "Southeast Asia–Indian Ocean–Suez Canal–Europe" route and the "East Asia–Pacific–U.S. West Coast" route. Together with the critical maritime chokepoints along them, these routes form the main structure connecting China to the global maritime trade network (Fig. 2a). Within this spatial configuration, the East China Sea and the South China Sea are China's principal maritime gateways. Each carries more than 64% of China's maritime imports and more than 43% of its maritime exports. Detailed statistics are provided in Supplementary Table 12. Beyond China's coastal waters, the Strait of Malacca is the most important international chokepoint for China-related cargo. It carries approximately 39% of import value and 27% of export value. The Bab el-Mandeb Strait, the Suez Canal, the Strait of Gibraltar, and the English Channel are widely recognized as global maritime chokepoints. They are also key nodes in China's trade, each carrying roughly 11–24% of China-related maritime cargo value. In addition, the Strait of Hormuz and the Bosporus Strait account for approximately 12% and 7% of China's maritime imports, respectively, while each carries only around 1% of its maritime exports. About 8% of China's maritime imports and 7% of its maritime exports pass through the Panama Canal, mostly to and from the Americas.

The Mining and Quarrying sector accounts for the largest share of China's maritime imports (Fig. 2b). Apart from the Strait of Gibraltar and the English Channel, mining and quarrying products make up more than 26% of cargo value at every major chokepoint. Its share is particularly high for trade passing through the South China Sea, the Strait of Malacca, the Strait of Hormuz and the Bosporus Strait. This distribution reflects China's strong dependence on resource-based imports from Asia and the Middle East (Zhou et al., 2020). Petroleum, chemical and non-metallic mineral products, electrical and mechanical equipment, and transport equipment also account for substantial shares at several chokepoints. On the export side, electrical and mechanical equipment accounts for the largest share of China's maritime exports, particularly at the Bab el-Mandeb Strait, the Suez Canal, the Bosporus Strait and the English Channel (Fig. 2c). This pattern reflects the importance of European economies as end markets for these products. Petroleum, chemical and non-metallic mineral products, textiles and apparel, and other manufactured goods come next at several chokepoints.

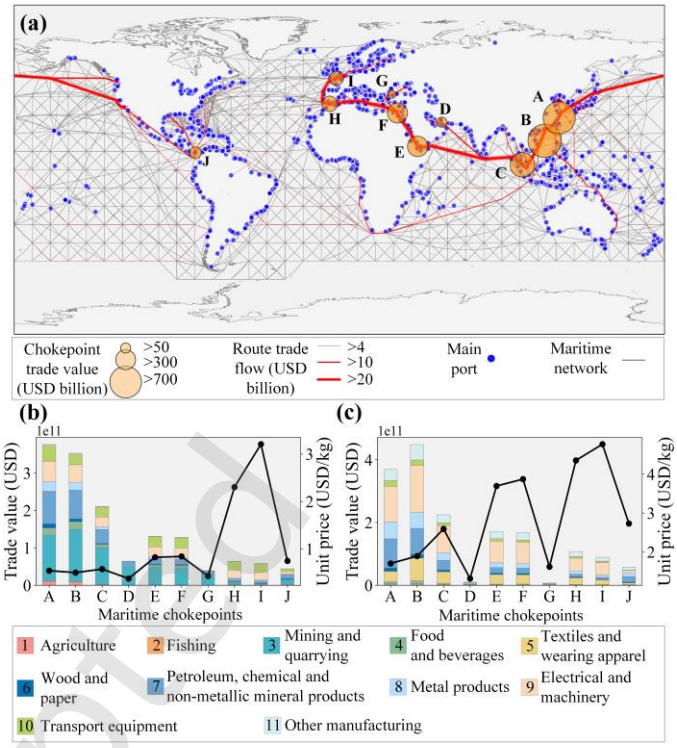

Fig. 2 China's maritime trade routes and trade structure at key maritime chokepoints. (a) Major maritime trade routes, trade volumes, and key maritime chokepoints traversed by China's maritime trade; trade volumes represent the combined value of imports and exports, measured in USD. (b–c) Sectoral composition and trade value of China's imports and exports at the key maritime chokepoints labeled A–J: A) East China Sea, B) South China Sea, C) Strait of Malacca, D) Strait of Hormuz, E) Bab el-Mandeb Strait, F) Suez Canal, G) Bosporus Strait, H) Strait of Gibraltar, I) English Channel, and J) Panama Canal. This figure is for illustrative purposes only.

3.2. Cost increases and trade contraction induced by chokepoint closures

Each of the ten chokepoints is closed in turn and treated as fully impassable. Ships cannot bypass the Strait of Hormuz or the Bosporus Strait by sea, so these two are left out of the rerouting-cost analysis. At the other eight, most affected routes can switch to another corridor, at a higher cost. Across these closure scenarios, rerouting increases average travel time by 12–342 hours and average shipping cost by approximately USD 0.17–3.46 million per affected route (annual flow). These cost increases could reduce the original trade flows by 3–49%.

Closure of the East China Sea, the Strait of Malacca or the English Channel has relatively small cost impacts. Rerouting adds approximately 300–1,120 km and 12–48 hours per affected route on average, and increases costs by USD 0.17–0.58 million (Figs. 3a–c). If the South China Sea is closed, affected vessels are rerouted through alternative passages such as the Makassar Strait or the Lombok Strait, causing delays of 91–96 hours and additional costs of USD 0.68–1.02 million. Closure of the Strait of Gibraltar or the Panama Canal has somewhat larger impacts, with delays of 206–224 hours and additional costs of USD 1.59–3.06 million. The largest impacts follow the closure of the Bab el-Mandeb Strait or the Suez Canal, which forces many vessels to reroute around the Cape of Good Hope. This diversion adds

Under Accepted

approximately 7,500–8,000 km, causes delays of 319–342 hours, and raises shipping costs by USD 2.68–3.46 million.

These estimates are the means of Monte Carlo simulations that account for uncertainty in vessel-type composition and unit shipping costs. The coefficients of variation (CVs) of total rerouting costs range from only 0.003 to 0.006 across chokepoints (Fig. 3d).

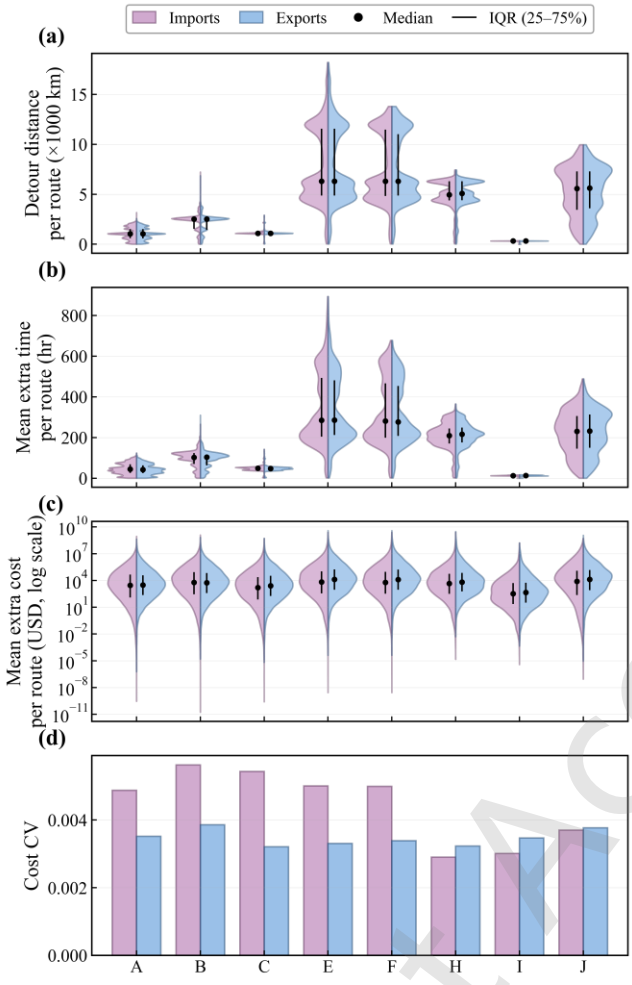

Fig. 3 Distributions of rerouting distance, time, cost, and cost variability across eight maritime chokepoints for China's imports and exports. (a) Rerouting distance per route. (b) Mean additional transit time per route in hours. (c) Mean additional shipping cost per route on a logarithmic scale. (d) Coefficient of variation (CV) of total rerouting cost. The letter labels of the eight chokepoints correspond to those in Fig. 2.

Differences in the composition of imported and exported goods lead to varying degrees of delays and costs. Averaged across all routes, the additional transit time is approximately 146 hours for imports and 140 hours for exports, a difference of around 4%. By contrast, the average cost increase per affected route is approximately USD 1.45 million for exports, around 13% higher than the USD 1.28 million estimated for imports. As shown in Section 3.1, imports are dominated by bulky, low-value resource commodities that are typically transported at lower speeds. Exports are more concentrated in high-value manufactured goods, whose cost increases are more sensitive to delays. Fig. 4 shows the contributions of individual sectors to additional shipping costs. On the import side (Fig. 4a), mining and quarrying (S3) accounts for the largest share (34%). Together with petroleum, chemicals, and non-metallic mineral products (S7), it accounts for about 49% of the total. On the export side (Fig. 4b), the additional cost is highly concentrated in electrical and machinery (S9, 40%), far exceeding other sectors.

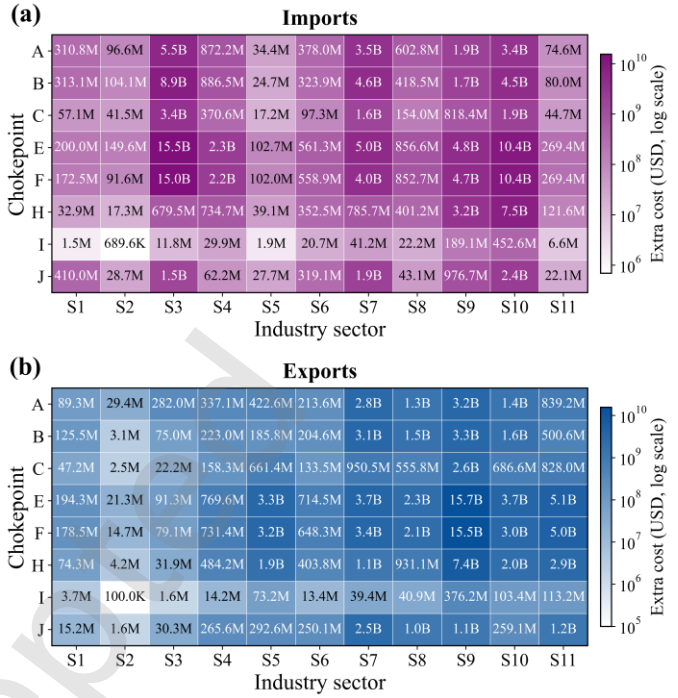

Fig. 4 Additional shipping costs by sector and chokepoint for China's imports and exports. Cells give the extra shipping cost of each sector at each chokepoint, summed over all rerouted routes. Values are Monte Carlo means in USD. K, M and B denote thousand, million and billion. Chokepoint letters and sector numbers as in Fig. 2.

Closure of a maritime chokepoint does more than increase transport costs. If the cost of rerouting exceeds what the cargo value can absorb, part of the trade flow becomes economically unviable. Fig. 5 shows the resulting trade contraction for each closure under several trade-cost elasticities. Greater trade contraction is generally associated with higher rerouting costs. Taking the import side with $\varepsilon = -4$ as an example, the closure of the Bab el-Mandeb Strait and the Suez Canal reduces trade by about 49% and 48%, respectively. The closure of the Strait of Gibraltar or the Panama Canal reduces trade by about 37% or 33%. Rerouting distances are relatively short for the South China Sea, the East China Sea and the Strait of Malacca. Their estimated trade contractions are about 19%, 11%, and 10%, respectively. The English Channel experiences the lowest rerouting costs and a trade contraction of only about 3%.

At every chokepoint, the estimated contraction is higher for imports than for exports, with differences ranging from approximately 0.6 to 7.9 percentage points. As noted above, China's imports mainly consist of bulk, low-value resource-based commodities. Additional detour costs have a more significant cost impact relative to the value of the goods. Exports are concentrated on high-value electrical and machinery products, the value of which far exceeds the increased transportation costs. Their trade therefore contracts less. The relative ranking of chokepoints by trade contraction remains broadly stable, although the magnitude of the estimated contraction is sensitive to the assumed trade-cost elasticity. Fig. 5a reports estimates over the range $\varepsilon \in [-6, -3]$. Because the behavioral adjustment of individual economies cannot be

Just Accepted

observed, this range is used as a parameter-uncertainty band representing different degrees of long-run trade adjustment; illustrative cases with lower elasticities are reported in Supplementary Table 9.

The amount of trade lost following a chokepoint closure depends on both the volume of affected trade and the corresponding trade-contraction rate. Figs. 5b–c divide the affected flows into trade maintained through rerouting at higher transport costs and trade forgone. Averaged across the eight closure scenarios, approximately 22% of affected import trade and 20% of affected export trade are forgone. The remaining 78% of imports and 80% of exports continue through alternative routes at higher costs.

The East China Sea, the South China Sea and the Strait of Malacca carry the largest volumes of affected trade. However, their trade-contraction rates are relatively low, because the added cost of the alternative routes is small relative to cargo value. The opposite pattern is found for the Bab el-Mandeb Strait and the Suez Canal. Although they affect smaller trade volumes, the high cost of rerouting pushes their contraction rates to nearly 50%. The absolute value of forgone trade at these chokepoints is therefore comparable to, or greater than, that at chokepoints carrying more trade. Chokepoint risk assessment needs to consider both trade volume and the cost of rerouting.

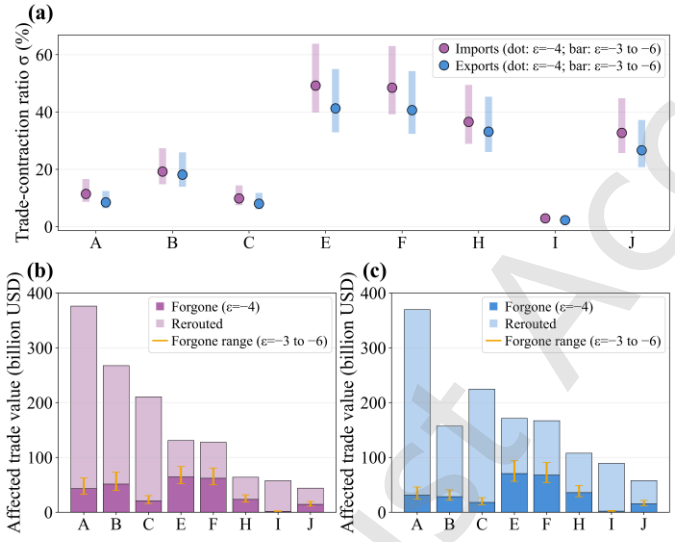

Fig. 5 Endogenous trade contraction and decomposition of forgone and rerouted trade at maritime chokepoints. (a) Trade-contraction ratio by chokepoint. (b–c) Decomposition of affected trade value for imports and exports.

For economies bordering semi-enclosed seas or enclosed gulfs, a single chokepoint may provide the only maritime connection to the open ocean. Its closure can therefore sever almost all external maritime trade. The Bosporus Strait connects the Black Sea to the Sea of Marmara. Its closure would cut virtually all maritime links between China and the Black Sea coastal states and their hinterlands, including Ukraine, Romania, Bulgaria and Georgia. For these economies, food and beverages account for 36% of the affected imports, followed by petrochemical products at 23%. Affected exports are dominated by electrical and machinery and by petroleum, chemical and non-metallic mineral products, which account for 36% and 34%, respectively.

The Strait of Hormuz is the only maritime link between the Persian Gulf and the open ocean. Its closure would virtually sever the maritime trade of Gulf economies such as the United Arab Emirates, Qatar, Kuwait, Iraq, and Bahrain with the rest of the world. For China, almost all affected imports are energy and raw materials: petrochemical and mining products make up 98% of them. Affected exports are mainly metal products, petrochemicals and electrical and mechanical equipment, which together account for 76%. These chokepoints are vital to the economic security of the countries that depend on them. The composition of the cargo passing through them also affects the economic stability of these countries' trading partners and of the wider global economy.

3.3. Global economic impacts of China-related trade disruptions

Closures of critical maritime chokepoints can transmit economic impacts through supply-chain networks and create systemic shocks across domestic and international sectors (Rousset and Ducruet, 2020). We start with how partner economies use China-related trade flows in production and consumption, then follow disruptions through cross-border industrial linkages, and finally sum the gross-output effects by closure scenario.

Importing economies use Chinese goods in two ways: for domestic final consumption and as inputs to their export production (Verschuur et al., 2022). The import impact indicator is highest in East Asia and the Pacific for both uses (Fig. 6a). In every region, more of these goods go to final consumption than to re-export. The median value for domestic consumption is approximately 1 to 3.42 times that for re-export. The ratio peaks at 4.54 in low-income economies, which mostly consume what they buy from China. Middle-income economies also direct much of these imports to domestic demand but re-export a sizeable part, in line with their place in intermediate processing. In high-income economies the two uses are closer in size (Fig. 6b).

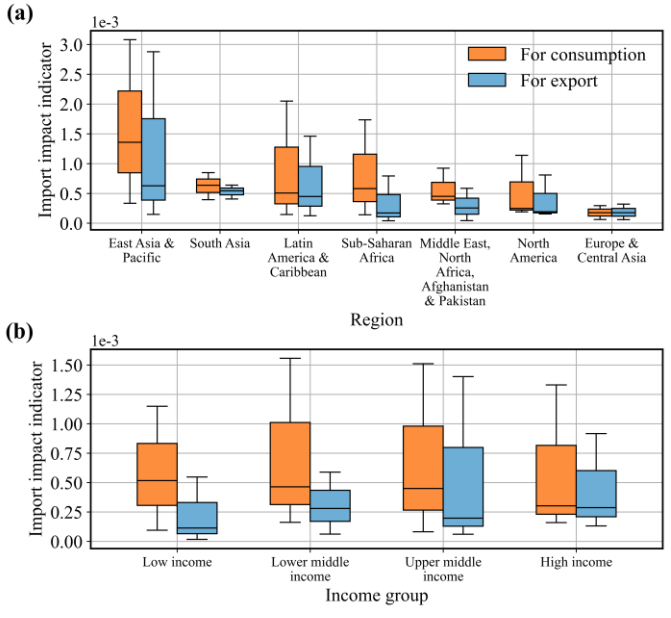

Fig. 6 Import dependence across regions and income groups. (a) Distribution of import impact indicators by region. (b) Distribution of import impact indicators by income group.

Furthermore, we examine the position of the relevant goods within the international cross-industry network. The export impact indicator shows that disruptions to China's import flows generate much stronger

Just Accepted

backward than forward effects in the affected economies. On the log scale (log1p), the median backward effect is about 3.60 times the median forward effect (Fig. 7a), because China mainly imports raw materials and intermediate inputs for its own processing and re-export chains; a disruption therefore hits supplier economies upstream. For Chinese exports the ratio is reversed, with the median forward effect about 3.51 times the backward effect (Fig. 7b). Much of what China exports is final goods, so a disruption tends to propagate downstream towards consumption and end use in importing economies.

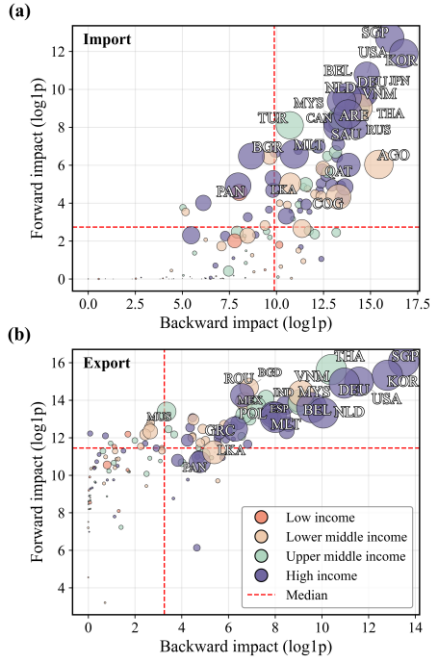

Fig. 7 Economic impacts of disruptions to trade flows with China across economies. (a–b) Forward (downstream) and backward (upstream) impacts of disruptions to China's import and export trade flows. Letters denote the ISO 3166-1 alpha-3 (ISO3) codes of the corresponding countries or regions.

The preceding analysis shows that trade-flow disruptions differ in both direction and intensity as they propagate through the industrial network. We next aggregate the affected trade flows by chokepoint to estimate the systemic effects associated with each closure. Figs. 8a–b show that cascading gross-output effects are concentrated at the South China Sea, the Bab el-Mandeb Strait and the Suez Canal. Together, these three chokepoints account for more than 52% of import-side cascading effects and nearly 66% of export-side effects. Effects associated with the remaining chokepoints are smaller and more evenly distributed. For individual chokepoint closures, under the baseline scenario ($\varepsilon = -4$), annual global gross-output effects on the import side range from approximately USD 9.5 to 289 billion, while those on the export side range from approximately USD 7 to 411 billion. Taking the median across all ten chokepoints, closure of a single chokepoint disrupts approximately USD 47 billion of China-related trade and is associated with USD 112 billion of gross output within China and a further USD 110 billion in other economies. The total global gross-output effect therefore amounts to approximately USD 220 billion.

The estimated effects are moderately sensitive to the assumed trade-cost elasticity. As $|\varepsilon|$ increases, the median cascading effect across chokepoints rises monotonically, from approximately USD 119 billion at $\varepsilon = -3$ to USD 166 billion at $\varepsilon = -6$ for imports, and from USD 72 billion to USD 134 billion for exports (Figs. 8a–b). Relative to the baseline scenario ($\varepsilon = -4$), this corresponds to a change of approximately −15% to +19% for imports and −23% to +42% for exports.

Dividing the gross-output effect by the value of disrupted trade gives the gross-output exposure multiplier. This multiplier measures the gross output linked to each unit of disrupted trade through backward and forward production linkages. As shown in Figs. 8c–d, each USD 1 of disrupted trade is associated with approximately USD 4.78 of global gross output on the import side and USD 4.70 on the export side. This combined indicator adds the backward (demand-side) component, about 2.5–2.8, and the forward (supply-side) component, about 1.9–2.3, each of which includes the disrupted flow itself as one unit of direct effect (Supplementary Table 8). Value-added effects are reported in Supplementary Tables 7–8.

The multiplier is robust. Across trade years, it ranges from 4.62 to 4.78. Even with extreme perturbations in the input–output coefficient (CV = 30%), its 95% confidence interval remains between 4.53 and 5.11 (see Supplementary Figs. 2 and 4). The uncertainty of trade-cost elasticity mainly affects the size of the shock, with an impact on the multiplier of no more than 0.1. This stability arises because the multiplier depends on the sectoral and partner composition of the disrupted trade and on the structure of production linkages, all of which change slowly.

This multiplier can be further divided into a domestic part and an international part. For import disruptions, every USD 1 of disrupted trade is associated with approximately USD 2.64 of gross output in the rest of the world, higher than the USD 2.14 in China. This reflects China's role as a major global consumer of intermediate goods and resource inputs. When China's imports are disrupted, the resulting decline in import demand will impact the economies of the supplying countries and their upstream production systems. The Strait of Hormuz is an exception. Its closure would place a larger share of the multiplier in China, because the energy and mineral resources passing through it are essential inputs to China's production system. In the event of an export disruption, a larger portion of the multiplier effect occurs within China. Every USD 1 of disrupted trade is associated with approximately USD 2.55 of gross output in China and USD 2.15 in the rest of the world. This is because export production in China is closely tied to domestic industries. Therefore, different trade resilience enhancement strategies need to be developed to address the different impact patterns of export and import disruptions.

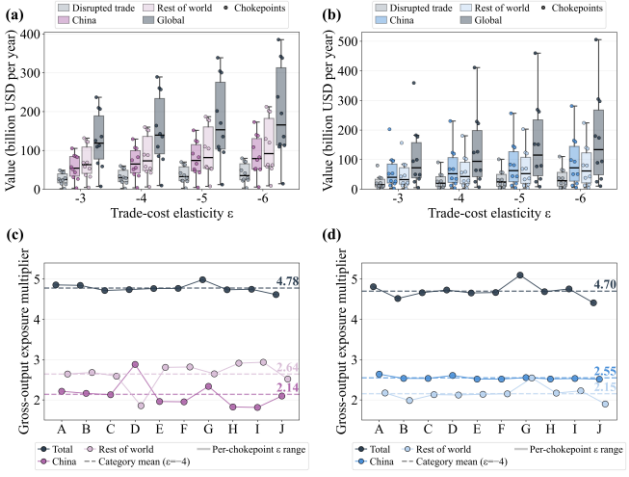

Just Accepted

Fig. 8 Gross-output effects and gross-output exposure multipliers associated with maritime chokepoint closures affecting China's imports and exports. (a–b) Disrupted trade and cascading gross-output effects in China, the rest of the world, and globally under different trade-cost elasticities for import and export disruptions; (c–d) Gross-output exposure multipliers for individual chokepoints and their mean values on the import and export sides. Chokepoint labels correspond to those in Fig. 2.

4 Discussion

4.1. Trade resilience and policy implications

Against a backdrop of slowing global economic growth, renewed trade protectionism and rising geopolitical uncertainty, strengthening the resilience of the global trading system while safeguarding national economic security has become a shared international challenge (World Bank, 2025; Zahoor et al., 2023). As the world's largest trader of goods and a major manufacturing hub, China is deeply embedded in global value chains and regional production networks. Its trade activities are therefore closely coupled with global production and consumption systems and have systemic implications for the functioning of international trade (Chu et al., 2025).

Our results show that closures of critical maritime chokepoints produce longer transport delays, higher trade-contraction ratios and stronger backward cascading effects on the import side of China's trade. Disruptions to China's imports not only threaten the stability of domestic production but also propagate upstream to external suppliers. To address these challenges, China can further advance its opening-up, forge partnerships with more entities, and enhance supply redundancy. It should encourage enterprises to establish production facilities in multiple overseas locations to diversify risk exposure. In parallel, by leveraging the advantages of its large domestic market, China can attract producers of advanced industrial products, critical components, and core equipment, thereby strengthening domestic supply capacity for essential goods.

Export-side disruptions exhibit a different pattern of vulnerability. High-value manufactured goods account for much of China's exports and contribute to larger rerouting-cost increases per route. Domestic industrial linkages also place more of the export-side multiplier within China. Continuity of export production therefore matters for both domestic industries and the markets they supply (H. Wang et al., 2024; Zhang et al., 2025). This requires China to strengthen the mutually reinforcing relationship between its domestic and international markets. While maintaining its export capacity, China should further tap into the potential of its domestic market and enhance enterprises' flexibility to shift export products to the domestic market when necessary. Meanwhile, enterprises should be encouraged to diversify their overseas markets and reduce dependence on a few export destinations.

China's long-term development experience shows that openness, cooperation, and mutual benefit are effective ways to maintain stability in international trade. Looking ahead, China should continue to share its development opportunities with the world and, leveraging its growing global economic influence, take a more proactive role in participating in and promoting the establishment of international collective risk management mechanisms.

4.2. Applicability and limitations of the findings

Our estimates of transport costs, trade contraction and economic impacts carry uncertainty from both the data and the model. We test three sources of it: how trade is allocated across ports, the inter-industry structure, and the year of data. Port-level allocation shares and input–output coefficients are perturbed, and the analysis is rerun with trade data for other years. We also cross-validate the results against independent external data. Detailed results are provided in the Supplementary Materials.

The results show that uncertainty in port-level trade allocation mainly affects the estimated trade volumes for China's coastal gateways in the East China Sea and the South China Sea. The reason is the uncertain split of trade between northern and southern Chinese ports (Supplementary Fig. 1). International chokepoints are hardly affected. Once ships reach open waters, trade from different ports tends to converge onto a few stable trunk routes. These allocation errors do not alter the relative ranking of the chokepoints. The modeled exposure estimates are also broadly consistent with several independent external statistics for the Strait of Hormuz, the Strait of Malacca, the Bosporus Strait, the Suez Canal and the Panama Canal (Supplementary Table 4). In addition, the estimated route distances have a mean error of only 1.09% relative to publicly available distance data for 15 representative routes, further supporting the reliability of the route-allocation results (Supplementary Table 5).

We run Monte Carlo simulations that randomly vary the input–output technical coefficients and the Ghosh output allocation coefficients, with a CV of 10–30% (Supplementary Fig. 2). The gross-output exposure multipliers remain robust across this range. They fluctuate more only at a few chokepoints, such as the Bosporus Strait and the Strait of Hormuz. At these chokepoints, trade volumes are smaller and the sectoral composition of trade is more concentrated. For the temporal dimension, we repeat the analysis using trade data for 2019, 2021, and 2024. The ranking of chokepoints by exposure share remains stable across years (Supplementary Fig. 3). The gross-output exposure multipliers range from 4.62 to 4.78 (Supplementary Fig. 4), and the distributions of rerouting costs and trade-contraction rates are also highly consistent. For 2024, data limits mean that trade flows are combined with the 2019 shipping network and input–output table, so this test reflects changes in trade scale and composition only, not in the network or in production linkages.

Nevertheless, the framework relies on several simplifying assumptions and may therefore deviate from real-world conditions. First, trade exposure at critical chokepoints is estimated using a cargo shortest-path model rather than observed vessel trajectories. Actual route choice is also shaped by factors such as weather, risk aversion, ship schedules, and congestion (Jang and Kim, 2022; Liu et al., 2025). Accordingly, the estimated additional costs reflect cost-minimizing rerouting. Second, the economic assessment uses a linear input–output model, which assumes fixed coefficients and applies a uniform elasticity of trade costs. As a result, the framework does not account for input or supplier substitution, price adjustments, inventory fluctuations, or shifts to alternative transport modes (Matsuyama et al., 2024). The estimated impacts should therefore be interpreted as a measure of risk exposure rather than as a prediction of actual losses. Third, the findings are based on a one-year disruption scenario. If a disruption lasts less than one year, the share of annual trade flows

Just Accepted

affected would be smaller; this reduction would not be strictly proportional, however, because some delayed goods could still be shipped later. Finally, the vessel and cost parameters used in the model are based on industry averages and currently exclude carbon emissions. Future work will focus on addressing these limitations.

5 Conclusion

This study develops an analytical framework that integrates trade statistics, maritime transport networks, and MRIO data. We apply this framework to assess the potential impacts of closures at ten major maritime chokepoints on China's trade and the global economy. The results show that the severity of a chokepoint closure depends not only on the volume of affected trade but also on rerouting costs and the availability of alternative routes. Consequently, even chokepoints with relatively low trade volumes may still constitute critical vulnerabilities if no alternatives exist or if rerouting proves prohibitively expensive. Beyond direct trade effects, the closure of chokepoints also triggers cascading effects through global industrial linkages. Disruptions to China's imports spread to external supplier economies, while disruptions to its exports are transmitted to China's domestic industries.

Overall, China is highly exposed to external supply shocks and also serves as a pivotal node through which trade disruptions can propagate globally. Therefore, safeguarding critical maritime chokepoints, improving the substitutability of transport routes, and deepening international coordination are crucial for enhancing the resilience of China's trade system and global supply chains.

Author contributions

Zhan'ao Zhao: Writing – original draft, Formal analysis, Methodology. **Kai Liu:** Writing – review & editing, Visualization, Conceptualization. **Xiaoyi Miao:** Software, Validation. **Jiawang Zhang:** Investigation, Data curation. **Ming Wang:** Supervision.

Replication and data sharing

The source codes and replication package are available on ETS at DOI: 10.26599/ETSD.2026.9190122.

Acknowledgements

This work was funded by the General Program of National Natural Science Foundation of China (No. 42377467), the National Key Research and Development Program of China (No. 2024YFC3808601) and the Fundamental Research Funds for the Central Universities (No. 2243300007). This work is part of the project "Climate Change and Systemic Risk Governance", which contributes to the implementation strategy of the UNESCO International Decade of Sciences for Sustainable Development (IDSSD, 2024–2033).

Declaration of competing interest

The authors declare that they have no known competing financial interests or personal relationships that could have appeared to influence the work reported in this paper.

Just Accepted

References

Arreyndip, N.A., 2025. The Russia–Ukraine conflict: A global impact assessment in the corn and wheat sectors. Agriculture 15(5), 550.

Balas, E.A., Balas, C.E., 2025. Maritime risk assessment: a cutting-edge hybrid model integrating automated machine learning and deep learning with hydrodynamic and Monte Carlo simulations. J. Mar. Sci. Eng. 13(5), 939.

Bergstrand, J.H., Egger, P., Larch, M., 2013. Gravity redux: estimation of gravity-equation coefficients, elasticities of substitution, and general equilibrium comparative statics under asymmetric bilateral trade costs. J. Int. Econ. 89(1), 110–121.

Berthou, A., Stumpner, S., 2024. Trade under lockdown. J. Int. Econ. 152, 104013.

Bo, A., Xie, Y., He, Z., Wang, C., Gou, Y., 2024. Maritime transportation security of strategic minerals: a case study of iron ore. Strategic Study of CAE 26(3), 142–151.

Chu, Z., Liu, G., Yang, J., 2025. Rethinking the semi-periphery: China's impact on global value chains and environment. Environ. Impact Assess. Rev. 115, 108033.

Davis, S.C., Dahal, P.M., Moore, A.M., Patwary, L., Boundy, R.G., 2026. Transportation Energy Data Book: Edition 41. Oak Ridge: Oak Ridge National Laboratory. https://tedb.ornl.gov.

Dirzka, C., Acciaro, M., 2022. Global shipping network dynamics during the COVID-19 pandemic's initial phases. J. Transp. Geogr. 99, 103265.

Duan, M., Yang, H., Lou, F., 2024. The impact of international shipping blockages on global economy and trade: simulation analysis of the Red Sea channel based on a general equilibrium model. Int. Econ. Trade Res. 40(10), 73–88.

Feyrer, J., 2021. Distance, trade, and income—The 1967 to 1975 closing of the Suez canal as a natural experiment. J. Dev. Econ. 153, 102708.

Gaulier, G., Zignago, S., 2010. BACI: international trade database at the product-level (the 1994–2007 version). CEPII Working Paper No. 2010-23. http://www.cepii.fr/PDF_PUB/wp/2010/wp2010-23.pdf.

General Administration of Customs of the People's Republic of China (GACC), 2025. Exceeding 43 trillion yuan! China's foreign trade hits a new record high in 2024. http://www.customs.gov.cn/customs/2025-01/14/article_2025121410060030365.html.

Grossman, G.M., Helpman, E., Redding, S.J., 2024. When tariffs disrupt global supply chains. Am. Econ. Rev. 114(4), 988–1029.

Halim, R., Kirstein, L., Merk, O., Martinez, L., 2018. Decarbonization pathways for international maritime transport: a model-based policy impact assessment. Sustainability 10(7), 2243.

Head, K., Mayer, T., 2014. Gravity equations: Workhorse, toolkit, and cookbook. In: Handbook of International Economics. Gopinath, G., Helpman, E., Rogoff, K., Eds. Amsterdam: Elsevier, 131–195.

Hoffmeister, O., Halim, R., Lazarou, N.J., Barnat, N., Cristallo, D., Englert, D., et al., 2022. Developing a global transport costs dataset for international trade. UNCTAD Research Paper No. 85. United Nations Conference on Trade and Development.

Jang, D., Kim, J., 2022. Development of ship route-planning algorithm based on rapidly-exploring random tree (RRT*) using designated space. J. Mar. Sci. Eng. 10(12), 1800.

Kang, H., Lee, K.M., Yang, J.S., 2024. The potential for cascading failures in the international trade network. PLoS One 19(3), e0299833.

Kazancoglu, Y., Ekinci, E., Mangla, S.K., Sezer, M.D., Ozbiltekin-Pala, M., 2023. Impact of epidemic outbreaks (COVID-19) on global supply chains: a case of trade between Turkey and China. Socio-Econ. Plan. Sci. 85, 101494.

Lee, P.T.W., Song, Z.Y., Chhetri, P., Shin, S.H., 2025. China's twin strategic development of iron-ore imports along the maritime silk road: Economic security and decarbonization of maritime industry. Ocean Coast. Manag. 260, 107483.

Li, D.Y.H., Jiao, J.B., Wang, S.Y., Zhou, G.H., 2025. The impact of global key shipping channel disruption on supply chains—case study of the grounding of Ever Given in the Suez Canal. Manag. Rev. 37(2), 237–248.

Ligteringen, H., Velsink, H., 2012. Ports and Terminals. Delft: VSSD.

Lin, F., Li, X., Jia, N., Feng, F., Huang, H., Huang, J., et al., 2023. The impact of Russia–Ukraine conflict on global food security. Glob. Food Secur. 36, 100661.

Liu, L., Zhang, M., Liu, C., Yan, R., Lang, X., Wang, H., 2025. Shipping map: an innovative method in grid generation of global maritime network for automatic vessel route planning using AIS data. Transp. Res. C: Emerg. Technol. 171, 105015.

Martínez, L.M., Kauppila, J., Castaing, M., 2015. International freight and related carbon dioxide emissions by 2050: new modeling tool. Transp. Res. Rec. 2477(1), 58–67.

Matsuyama, R., Sugimura, Y., Shibasaki, R., Tran, T.T.T., 2024. Scenario analysis on CO2 emission reductions in hinterland transport of Japan through intermodal logistics network simulation. J. Clean. Prod. 458, 142503.

Mesa-Arango, R., Narayanan, B., Ukkusuri, S.V., 2019. The impact of international crises on maritime transportation based global value chains. Netw. Spat. Econ. 19(2), 381–408.

Mi, K., Zhuang, R., 2022. Producer services agglomeration and carbon emission reduction—an empirical test based on panel data from China. Sustainability 14(6), 3618.

Notteboom, T., Haralambides, H., Cullinane, K., 2024. The Red Sea crisis: ramifications for vessel operations, shipping networks, and maritime supply chains. Marit. Econ. Logist. 26(1), 1–20.

Peng, Z., Zhao, B., Zhong, X., Deng, Y., Zheng, B., 2025. Strategies for China's participation in overseas strategic fulcrum ports from the perspective of the port value chain. Port Waterway Eng. (6), 13–22.

Pratson, L.F., 2023. Assessing impacts to maritime shipping from marine chokepoint closures. Commun. Transp. Res. 3, 100083.

Just Accepted

Rousset, L., Ducruet, C., 2020. Disruptions in spatial networks: a comparative study of major shocks affecting ports and shipping patterns. Netw. Spat. Econ. 20(2), 423–447.

Simonovska, I., Waugh, M.E., 2014. The elasticity of trade: estimates and evidence. J. Int. Econ. 92(1), 34–50.

Tan, Y., Steinberg, D., McDowell, D., 2025. Global economic influence and domestic regime support: evidence from China. Rev. Int. Polit. Econ. 32(1), 202–225.

Tang, H., Zheng, X., 2024. How did China's zero Covid policy affect its exports? Rev. Int. Econ. 32(2), 545–573.

Verschuur, J., Koks, E.E., Hall, J.W., 2022. Ports' criticality in international trade and global supply-chains. Nat. Commun. 13(1), 4351.

Verschuur, J., Lumma, J., Hall, J.W., 2025. Systemic impacts of disruptions at maritime chokepoints. Nat. Commun. 16(1), 10421.

Wan, Z., Su, Y., Li, Z., Zhang, X., Zhang, Q., Chen, J., 2023. Analysis of the impact of Suez Canal blockage on the global shipping network. Ocean Coast. Manag. 245, 106868.

Wang, H., Wu, Y., Zhu, N., 2024. Spatio-temporal heterogeneity of China's import and export trade, factors influencing it, and its implications for developing countries' trade. PLoS One 19(4), e0300307.

Wang, J., Wang, X., Feng, Y., Cao, Y., Guo, Z., Liu, Z., 2023. Assessing the connectivity reliability of a maritime transport network: a case of imported crude oil in China. J. Mar. Sci. Eng. 11(8), 1597.

Wang, L., 2015. Maritime strategy passage impact on China's economic security and countermeasures. J. Econ. Shanghai Sch. 13(1), 146–156.

Wang, N., Dong, L.L., Wu, N., Yan, H., 2016. The change of global container shipping network vulnerability under intentional attacks. Acta Geogr. Sin. 71(2), 293–303.

Wang, W.L., Zeng, X.J., 2026. Research on China's food trade and food security. World Reg. Stud. 35(2), 114 – 128.

Winter, M., Scholz, J., 2024. Spatio-temporal spread of disruptions in interconnected supply networks. AGILE: GIScience Ser. 5, 53.

World Bank, 2025. Global Economic Prospects, June 2025. https://thedocs.worldbank.org/en/doc/8bf0b62ec6bcb886d97295ad930059e9-0050012025/global-economic-prospects-june-2025.

Xiao, R., Xiao, T., Zhao, P., Zhang, M., Ma, T., Qiu, S., 2024. Structure and resilience changes of global liquefied natural gas shipping network during the Russia–Ukraine conflict. Ocean Coast. Manag. 252, 107102.

Xiao, Z., Bai, X., 2022. Impact of local port disruption on global container trade: an example of stressing testing Chinese ports using a D-vine copula-based quantile regression. Ocean Coast. Manag. 228, 106295.

Xie, Y.S., He, T.K., Yi, W., Peng, X., Liu, H., 2023. China's iron ore shipping import pattern and risk assessment. J. Nat. Resour. 38(11), 2741–2756.

Xiong, Y., Wu, S., 2021. Real economic benefits and environmental costs accounting of China–US trade. J. Environ. Manage. 279, 111390.

Yan, R., Wang, S., Zhen, L., Laporte, G., 2021. Emerging approaches applied to maritime transport research: past and future. Commun. Transp. Res. 1, 100011.

Zahoor, N., Wu, J., Khan, H., Khan, Z., 2023. De-globalization, international trade protectionism, and the reconfigurations of global value chains. Manag. Int. Rev. 63(5), 823–859.

Zamani, O., Farzanegan, M.R., 2026. Global food security rests on the Strait of Hormuz. Nat. Food 7, 301.

Zhang, L., Zhang, X., Yao, Y., Sun, P., Liu, Z., 2025. High-level opening-up and enterprise innovation resilience: evidence from a quasi-natural experiment of China's belt and road initiative. China Econ. Rev. 93, 102485.

Zhou, Q., He, Z., Yang, Y., 2020. Energy geopolitics in Central Asia: China's involvement and responses. J. Geogr. Sci. 30(11), 1871–1895.

Zhu, W., Liu, K., Wang, M., Ward, P.J., Koks, E.E., 2022. System vulnerability to flood events and risk assessment of railway systems based on national and river basin scales in China. Nat. Hazards Earth Syst. Sci. 22(5), 1519–1540.

Zhu, X., Mao, Z., Qu, J., Zhang, Z., 2024. Historical logic and maritime cultural foundation of China's initiative of building a maritime community with a shared future. Front. Mar. Sci. 11, 1362399.

JSE Accepted

Author biography



Zhan'ao Zhao is a Ph.D. student at the School of National Safety and Emergency Management, Beijing Normal University. His research interests focus on coupled risk assessment of transportation chains and supply chains under major emergency events.



Kai Liu received her Ph.D. degree in Civil Engineering from KU Leuven, Belgium, in 2010. She is currently a Professor and Ph.D. Supervisor at Beijing Normal University and serves as the Dean of the School of National Safety and Emergency Management. She is a recipient of China's National High-Level Young Talents Program. Her research interests focus on climate change, urban safety, and systemic disaster risk. She also serves as an Executive Council Member of the China Association for Public Safety Science and Technology and as an expert for the Beijing Municipal Emergency Management Bureau.



Xiaoyi Miao is a Ph.D. student at the School of National Safety and Emergency Management, Beijing Normal University. Her research interests include climate change and urban safety, critical infrastructure safety, and risk assessment of extreme climate-related disasters.



Jiawang Zhang is a Ph.D. student at the School of National Safety and Emergency Management, Beijing Normal University. His research interests include national security and systemic risk.



Ming Wang received his Ph.D. degree in Structural Engineering from the Department of Civil and Environmental Engineering, University of Maryland, USA, in 2006. He joined Beijing Normal University in 2008 and was promoted to Professor in 2013. He is currently a Vice President of Beijing Normal University. His research focuses on systemic risk in national security. He also serves as a Member of the Expert Committee of the National Disaster Reduction Commission of China, a Member of the Discipline Review Group (National Security Studies) of the Academic Degrees Committee of the State Council, and holds leading technical roles in the First National Comprehensive Risk Survey of Natural Disasters.

Just Accepted